Niobium self-diffusion*

R. E. Einziger,† J. N. Mundy, and H. A. Hoff
Materials Science Division, Argonne National Laboratory, Argonne, Illinois 60439
(Received 1 August 1977)

The diffusion of ^{95}Nb in niobium has been measured between 1353 and 2693 K. The data showed nonlinear Arrhenius behavior and fit the expression $D = [8 \times 10^{-3} \exp(-3.62\ \text{eV/kT}) + 3.7 \exp(-4.54\ \text{eV/kT})]$ $\text{cm}^2\text{sec}^{-1}$. The data are interpreted in terms of a single-vacancy–divacancy mechanism. The effect of oxygen on niobium self-diffusion was measured over the temperature range 1750–2690 K. There was no measurable difference in the diffusion coefficient obtained from samples with 500-wt-ppm O_2 and samples with less than 10-wt-ppm O_2.

I. INTRODUCTION

In the past ten years there has been an increasing amount of evidence that measurements of self-diffusion in some metals show nonlinear Arrhenius behavior.[1-8] The dominating theories[9-13] have explained the curvature in terms of a single-vacancy–divacancy mechanism contributing simultaneously to diffusion. For the face-centered-cubic (fcc) metals Al, Ni, Au, Ag, and Cu, analyses[11,14-16] have shown that at all temperatures below the melting point (T_m) the high-temperature mechanism contributes less to diffusion than the low-temperature mechanism. (Recent measurements of nickel self-diffusion indicate no curvature.[17]) For the body-centered-cubic (bcc) metals β-Ti, β-Zr, Na, and K, analyses[4-8] have shown that at temperatures above approximately $0.9T_m$ the high-temperature mechanism contributes more to diffusion than the low-temperature mechanism. The domination of the high-temperature diffusion mechanisms near the melting points of some bcc metals would suggest that curved Arrhenius plots might be more readily observed for diffusion measurements of bcc metals.

At the start of the present investigation, nonlinear Arrhenius behavior in bcc metals had been observed in two so-called "anomalous" bcc metals, β-Ti and β-Zr, and two alkali metals, Na and K. The high-melting-point bcc metals of groups V and VI have shown linear Arrhenius behavior,[18-22] with the exception of vanadium,[23-25] which all workers have described by separate linear Arrhenius plots in two distinct temperature ranges. Recent vanadium measurements[25] can also be interpreted in terms of two mechanisms operating simultaneously over the measured temperature range. The observation of curved Arrhenius plots in bcc metals with high melting points is made difficult by uncertainties in the temperature measurement. Measurements of self-diffusion in chromium[20] (group VI, $T_m = 2126$ K) showed no curvature, but as mentioned above, measurements in another metal with nearly the same melting point—vanadium (group V, $T_m = 2163$ K)—curvature was found. For this investigation, we have chosen the bcc metal with the next highest melting temperature above vanadium: that is, niobium (group V, $T_m = 2741$ K).

Niobium appeared to be an ideal candidate with which to make accurate self-diffusion measurements in a group-V bcc metal over a wide temperature range. Sectioning techniques[26,27] appeared to be available to allow diffusion measurements to values as low as 10^{-18} $\text{cm}^2\,\text{sec}^{-1}$, and the high specific activity of ^{95}Nb ensures that the thin-film condition for diffusion can be maintained. A large number of niobium self-diffusion measurements have been made,[18,28-31] but only Lundy *et al.*[18] made measurements over a wide temperature range (0.4 T_m to T_m). Lundy's measurements showed a linear Arrhenius behavior within the scatter of the data.

Measurements of self-diffusion in α-Fe[32] indicated that the magnitude of the diffusion coefficient was strongly dependent on the interstitial oxygen content of the iron. The iron with the lower oxygen content had the lower diffusion coefficient. The effect of oxygen content was large, which suggests that similar effects should be observable in other bcc metals. Niobium has a high affinity for oxygen, so the effect of oxygen on niobium self-diffusion should be investigated. The previous work[18] had seen no effect, but the annealing environments used in those[18] experiments (high-purity argon or a vacuum of ~1.3 mPa) would have ensured that oxygen levels were well above the point where the effects of oxygen might be observed. The diffusion measurements for iron[32] and measurements of void swelling[33] and yield strength[34] for niobium indicate that the major effect is to be found below a level of approximately 100 wt. ppm of oxygen. The diffusion measurements reported here were made on niobium samples with

oxygen contents of ~500 wt. ppm and <100 wt. ppm to look for an enhancement effect. Sample preparation was clearly critical and will be discussed in detail.

II. EXPERIMENTAL METHODS

The basic method used was to observe the diffusion of a thin surface layer of radiotracer by sectioning. The solution of the diffusion equation for these experimental conditions is

$$C(x) = [S/(\pi Dt)^{1/2}] \exp(-x^2/4Dt) , \quad (1)$$

where $C(x)$ is the specific activity of the tracer at a distance x from the surface; t is the time of anneal; D is the diffusion coefficient; and S is the tracer concentration per unit area at $x = 0$ and $t = 0$.

A. Preparation of niobium crystals

1. Growth of large interstitially pure single crystals

Niobium (Marz grade) was obtained from the Materials Research Corporation in the form of 6.4- and 9.5-mm-diam rod. The company's analysis showed the major substitutional impurity to be tantalum (<300 wt. ppm). The effect of substitutional impurities on self-diffusion is well known known,[35,36] and the tantalum content has an insignificant effect. Even though the contribution of tantalum to the niobium resistivity is only one-tenth of that for the same amount of oxygen,[37] at very low interstitial levels the tantalum becomes a major contributor to the residual resistivity. To allow use of resistivity ratio measurements as a test of niobium purity, the tantalum content of the niobium used in this work was determined by activation analysis. The content was ~150 wt. ppm which limited the ultimate residual resistivity ratio to 2000.

Single crystals were grown by the recrystallization process from 64-mm-long bars of MRC Marz-grade polycrystalline niobium that had been well stressed. The bars were annealed for 5 h at 1870 K in an atmosphere of oxygen at 3×10^{-4} Pa to remove interstitial carbon. This treatment left approximately 500 wt. ppm of oxygen in the samples. After the vacuum system was pumped down and the sample was baked, the sample temperature was raised to 2270 K. Initial outgassing made the pressure rise to the low 10^{-6}-Pa scale, but it rapidly dropped into the 10^{-7}-Pa region. A 40-h anneal was made with an ultimate pressure of 1×10^{-7} Pa. For both diameter bars, the familiar bamboo structure resulted in grains approximately 13-mm long. The grain position could be determined by the thermal etching that occurred at the grain boundaries.

2. Analysis for sample purity

Samples were cut off the ends of each bar for analysis. Vacuum-fusion analysis indicated less than 50 wt. ppm of interstitial impurity.

Niobium is superconducting at the liquid-helium temperatures at which the resistivity ratio measurements to test for purity were to be taken. The magnetic fields necessary to suppress the critical temperatures for these large bars were not available in a liquid-helium cryostat at Argonne. The size and shape of a sample dictates the time at temperature and vacuum necessary to achieve any desired interstitial purity. As a result, samples of different size and shape can be annealed with different time-at-temperature cycles to give the same interstitial purity. Wire-sample standards cleaned with time-at-temperature anneal conditions homologous to those for metal bars indicated a residual resistivity ratio of greater than 1000, which corresponds to 25 at. ppm or less total interstitial impurity for samples containing 150 wt. ppm of tantalum impurity. This is probably closer to the actual total interstitial content of the bar than the 50 wt. ppm determined by fusion analysis. Calculations by Strongin *et al.*[38] for the time-at-temperature conditions used to anneal the wire standards, predict an interstitial content $(O + C + N)$ of approximately 1 at. ppm total interstitial in the wire.

3. Sample preparation

Samples were cut from the large recrystallized grains on a Buehler low-speed diamond saw. The samples to be sectioned by grinding were polished through 4/0 grit SiC paper and lightly etched in a HNO_3-HF solution. Laue x-ray pictures confirmed the single-crystal nature of the samples. Samples to be sectioned by anodizing were further polished through 0.05-μm alumina grit on a vibratory polisher. After the diffusion anneals, some of the samples were cut on the diamond saw, using ethyl alcohol lubricant, and sent for analysis to see if there was additional oxygen pickup during the diffusion anneal.

B. Radioisotope

Carrier-free ^{95}Nb as niobium oxylate in oxalic acid was purchased from Oak Ridge National Laboratory (ORNL). The isotope contained approximately 0.2–0.8 at. % of ^{95}Zr as an impurity at the time of separation (ORNL specification). This level was confirmed to within a factor of two by a two-exponential fit to half-life measurements made over the course of a year on one batch of the isotope and by counting selected isotope samples with

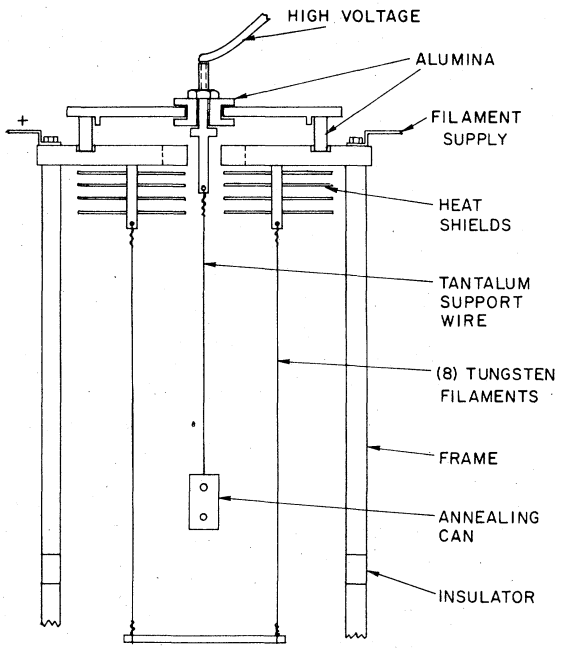

FIG. 1. Ultrahigh-vacuum electron-beam furnace.

a germanium detector. Due to the difference in half lives [$T_{1/2}(^{95}\mathrm{Nb}) = 35$ day] and [$T_{1/2}(^{95}\mathrm{Zr}) = 65$ day], the ^{95}Zr grew in concentration relative to the ^{95}Nb. Since separations at ORNL were done only twice a year, some diffusion anneals were made with as much as 1.5-at.% ^{95}Zr impurity. Initial diffusion anneals indicated a "tail" on the concentration profile, which could be attributed to this small amount of zirconium. The analysis of these tails is discussed in the following paper.[39] Attempts at in-house purification of the isotope resulted in an increased oxalic acid level, which hampered the dropwise deposition of the isotope onto the sample. A flaky powder that adhered very poorly to the sample resulted from the high oxalic acid content.

The isotope had high enough specific activity so that thin-film conditions ($<0.1\sqrt{Dt}$) were not violated on any of the anneals. At the start of the anneal, the oxalic acid converts to Nb and O_2 and the oxygen quickly effuses out of the anneal can (see Fig. 1). Even if all the O_2 from the oxalic acid entered the sample, at all annealing temperatures the niobium-to-oxygen diffusion ratios were such that the oxygen would have equilibrated over the entire sample so that its bulk content was only a few at. ppm.

C. Diffusion anneals

The oxygen content of the samples was controlled by making all the anneals in an ultrahigh-vacuum electron-beam furnace patterned after Birnbaum.[40] (See Fig. 1.) The filament cage was made of eight tungsten wires symmetrically placed around the sample to minimize azimuthal temperature gradients in the samples. The samples were hung from a high-voltage tantalum wire. When heated, the filaments emitted electrons that were accelerated toward the sample by the high voltage. The electron bombardment heated the samples.

For optimum operation, the new filaments were outgassed for a few hours in an ultrahigh vacuum at approximately 2470 K. After a bake, the system was capable of reaching 2870 K at a pressure of 2×10^{-8} Pa. There was little chamber outgassing, since only the sample and the preannealed filaments become hot. The warmup time to temperature could be less than a minute, because there is only a small thermal mass to heat. The fast warmup is an advantage in defining the anneal time for the diffusion measurements, and the low outgassing is advantageous when the oxygen content of the sample is critical. The disadvantage of such a system was the presence of a temperature gradient along the length of the sample can (Fig. 2), which ranged from 200 K at high temperatures to 70 K at 1770 K. Most of this gradient was across the gaps between the samples and not across the samples themselves. This was shown by a temperature scan on the surface of the can.

All anneals were done in either ultrahigh vacuum or in an oxygen atmosphere adjusted for the anneal temperature so that the steady-state oxygen content in the samples was maintained at the desired level. The time-at-temperature conditions

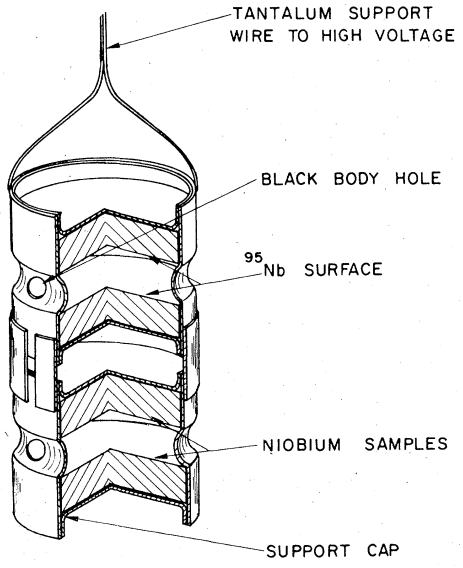

FIG. 2. Sample configuration for diffusion anneals.

were chosen so that the penetration of the isotope into the sample was much smaller than the thickness of the sample.

D. Sample configuration and temperature measurement

To eliminate much of the scatter in the previous data[18] due to uncertainties in the knowledge of the temperature, the temperature had to be known to ±20 K at 2470 K, ±10 K at 1770 K, and ±2 K at 1270 K. High-temperature thermocouples [W(26-at. % Re)–W(5-at. % Re)] are not this accurate, can show hysteresis, and are difficult to calibrate. At lower temperatures where thermocouples can be used, other problems occur.[41]

Manual disappearing-filament optical pyrometry was used for all temperature measurements in this work. The transmission coefficient of the sight port was corrected by calibrating the pyrometer through the port with a standard tungsten lamp before and after each run. This also allowed the determination of any metallic buildup on the window. None was observed.

The emissivity is dependent on the roughness of the material surface and the temperature of the sample; its value for niobium was not known well enough to correct to the necessary accuracy. The sample configuration, using two samples shown in Fig. 2, was chosen to meet the requirements for accuracy of temperature measurement. The samples formed the main part of a blackbody cavity of 99.9% quality.[42,43] This arrangement, by eliminating the error due to the unkown emissivity of the niobium surface and by giving the average temperature of the blackbody hole,[51] allowed the necessary accuracy to be obtained.

E. Sectioning

The sample sides were removed to a depth of $8\sqrt{Dt}$ to eliminate the effect of surface diffusion. For anneal conditions above 1720 K, sections were removed by precision parallel grinding on either 600 or 4/0 grit paper. The sample was weighed between each section removal to determine the section mass. Sections as thick as 20 μm or as thin as 0.5 μm could be taken by this technique. The limiting factor is the ability to accurately determine the weight change of the sample.

Anodizing has been used for taking thin sections of a number of metals. For serial sectioning, a suitable anodizing solution must be found which allows the oxide layer to be easily stripped. Since the surface could not be electropolished prior to annealing due to possible oxygen contamination, the method used by Lundy *et al.*[18,26,27] was not suitable for this work.

A modification of the Arora-Kelly technique[44] using a 3:1 ethyl sulfate-sulfuric acid solution for anodizing and a saturated KOH solution for stripping was used in this project. The sample was weighed before and after anodizing. The thickness of the anodized layer is determined by the voltage and current used for anodizing. The section thickness was determined from the average weight per section, the measured surface area, and the density of the niobium.

F. Counting

All sections were counted to a minimum of 10^4 counts in a NaI welltype counter. No correction for the $^{95}Zr-^{95}Nb$ decay over the counting period was made, since this was negligible for the 3-h period involved. The parent-to-daughter decay from the time of the anneal to the time of counting was accounted for; the method for determining this correction is described elsewhere.[39]

III. EXPERIMENTAL RESULTS

In most cases the penetration profiles obtained by grinding (Fig. 3) were straight over two and one-half to three orders of magnitude in activity and then began to show tails. These tails were present even in the anneals at temperatures near the melting point. In those profiles where the scatter in the data was sufficiently small and the ^{95}Nb isotope sufficiently old, the data allowed a

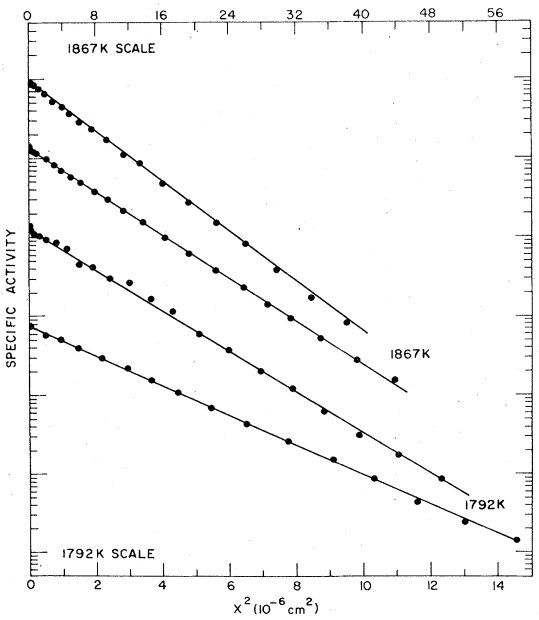

FIG. 3. Concentration profiles of ^{95}Nb in niobium obtained by grinding. Specific activities in arbitrary units.

two-exponential fit to be made and the diffusivities of ^{95}Nb and ^{95}Zr in niobium to be obtained. In general, the fits were excellent and the data agreed well with the data for Zr diffusion in niobium obtained from codiffusion of two isotopes reported in the next paper.[39] The two-exponential fit tended to lower the self-diffusion coefficient obtained from the one-exponential fit of the "straight-line" section of the profile, by 5% to 10%.

A typical penetration profile obtained by anodizing is shown in Fig. 4. The initial points of high value near the sample surface were caused by a residual-oxide layer that resulted from incomplete dissociation of the oxide formed from the ^{95}Nb isotope deposition. This oxide was not readily removed by the KOH stripping solution and came off slowly in the first half-dozen sections. It was removed from later profiles by hand polishing the surface to reduce the residual surface-oxide coverage to less than 10% of the surface area. The tail on each profile was assumed to result from both short-circuit diffusion and the high diffusivity of ^{95}Zr. The error in the diffusion coefficient obtained from the deconvolution of the anodizing profile was approximately 25%.

The two samples annealed at each blackbody temperature showed different values for the diffusion constant. It was known from relative surface-temperature scans that there was a temperature gradient along the annealing can, with the bulk of the gradient occurring across the gaps between the samples. In all cases the hotter sample of each

TABLE I. Diffusion of ^{95}Nb in niobium as a function of temperature.

D (cm^2 sec^{-1})	D_{avg} (cm^2 sec^{-1})	T (K)	Time (sec)	Oxygen content [a] and sectioning method
1.69×10^{-8} 1.13×10^{-8}	1.41×10^{-8}	2695	9.73×10^{2}	Doped, grinding
6.31×10^{-9} 5.24×10^{-9}	5.77×10^{-9}	2574	2.61×10^{3}	Doped, grinding
5.81×10^{-9} 3.89×10^{-9}	4.85×10^{-9}	2554	9.73×10^{2}	Clean, grinding
2.38×10^{-9} 1.66×10^{-9}	2.02×10^{-9}	2450	7.86×10^{3}	Doped, grinding
1.75×10^{-9} 1.22×10^{-9}	1.48×10^{-9}	2407	2.61×10^{3}	Doped, grinding
9.15×10^{-10} 8.62×10^{-10}	8.89×10^{-10}	2360	1.04×10^{4}	Clean, grinding
4.92×10^{-10} 3.20×10^{-10}	4.05×10^{-10}	2281	7.86×10^{3}	Doped, grinding
3.31×10^{-10} 2.49×10^{-10}	2.90×10^{-10}	2244	5.94×10^{3}	Doped, grinding
2.90×10^{-10} 1.71×10^{-10}	2.30×10^{-10}	2212	1.04×10^{4}	Clean, grinding
8.59×10^{-11} 6.66×10^{-11}	7.63×10^{-11}	2108	5.94×10^{3}	Doped, grinding
4.86×10^{-12} 4.16×10^{-12}	4.51×10^{-12}	1867	3.28×10^{5}	Doped, grinding
1.80×10^{-12} 1.56×10^{-12}	1.68×10^{-12}	1810	3.62×10^{5}	Clean, grinding
1.81×10^{-12} 1.31×10^{-12}	1.56×10^{-12}	1792	3.28×10^{5}	Doped, grinding
8.75×10^{-13} 7.55×10^{-13}	8.15×10^{-13}	1766	3.63×10^{5}	Clean, grinding
5.19×10^{-13} [b] 4.62×10^{-13}	4.90×10^{-13}	1738	1.63×10^{3}	Clean, anodizing
1.26×10^{-13} 7.09×10^{-14}	9.46×10^{-14}	1614	9.02×10^{2}	Clean, anodizing
1.07×10^{-14}	1.07×10^{-14}	1517	3.92×10^{3}	Clean, anodizing
3.87×10^{-15} 2.86×10^{-15}	3.33×10^{-15}	1446	2.50×10^{4}	Clean, anodizing
3.84×10^{-16}	3.84×10^{-16}	1354	1.80×10^{5}	Clean, anodizing

[a] "Doped" samples contained 500–800 wt. ppm of O_2, and "clean" samples <50 wt. ppm O_2.
[b] Profile questionable; value probably low.

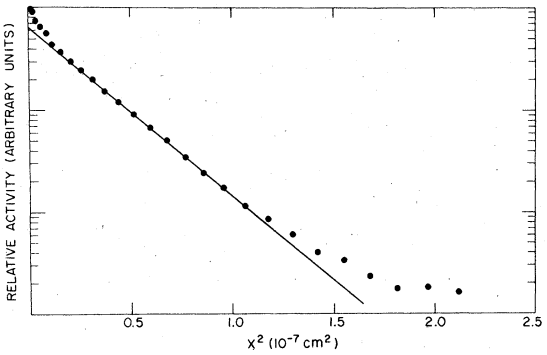

FIG. 4. Concentration profile of ^{95}Nb in niobium obtained by anodizing.

pair had the higher diffusion constant.

The data from the concentration profiles were least-squares fitted to obtain the values of the diffusion coefficients given in Table I and shown in Fig. 5. In Table I, all the average diffusion coefficients, except those for 1354 and 1517 K, were taken as the geometric average of two diffusion coefficients measured at the average blackbody temperature given in the third column. At 1354 and 1517 K, only one of the samples from each of the pairs could be sectioned, so the listed value

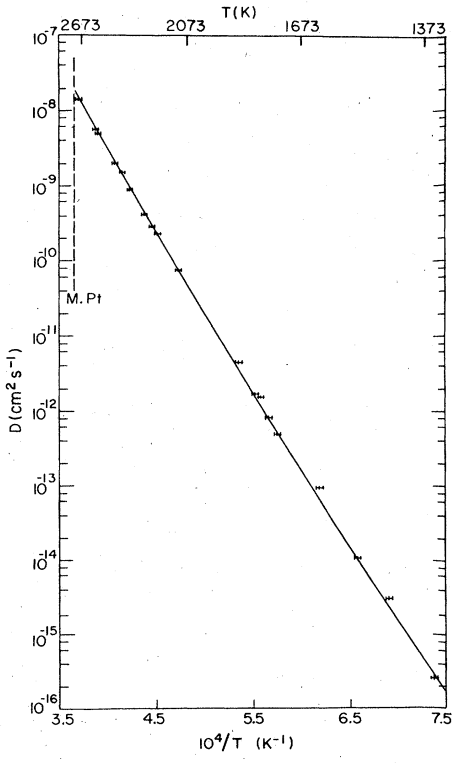

FIG. 5. Diffusion of ^{95}Nb in niobium as a function of temperature.

is the actual measured diffusion coefficient within the experimental error of ±25% found for the anodizing profiles. The largest error was in the measurement of temperature and had the values given in Sec. IID.

As can be seen in Fig. 5, the Arrhenius line shows curvature, and a two-exponential fit to the data gave the following relation

$$D = [8 \pm 3 \times 10^{-3} \exp(-3.62 \pm 0.09 eV/kT) + 3.7 \pm 0.3 \exp(-4.54 \pm 0.01 eV/kT)] \text{ cm}^2\text{sec}^{-1}.$$

IV. DISCUSSION

A. Effect of oxygen on self-diffusion in niobium

The considerable care that was exercised in examining whether the presence of oxygen affected the measurements of self-diffusion in niobium was strongly predicated by the results of Irmer and Feller-Kniepmeier[32] on self-diffusion in iron. There are many errors in this iron work but they would not account for the large difference (a factor of 40) between diffusion coefficients measured in samples with low- and high-interstitial impurity content. Recent measurements which compared self-diffusion in the same clean samples with iron that had an oxygen content in excess of 100 wt. ppm showed no difference in the diffusion coefficients.[45]

As can be seen from Table I and Fig. 5, varying the oxygen content of the niobium samples from 500 wt. ppm to less than 10 wt. ppm did not influence the self-diffusion coefficient in the measured temperature range 1740–2695 K [$(0.65–0.98)T_m$]. A strong influence of oxygen might be expected if niobium self-diffusion occurred by an oxygen-vacancy pair mechanism. Except at the highest temperatures, the oxygen would be in much greater concentration than the vacancies. Since all the vacancies would already be tied up with oxygen, the oxygen content would have to be reduced below the concentration of vacancies to initiate an effect on self-diffusion. The oxygen effect in iron self-diffusion was observed at lower homologous temperatures ($0.58T_m$ to $0.65T_m$) as was the oxygen effect in void swelling[33] and yield strength.[34] A comparison of the diffusion rate in oxygenated and "pure" niobium samples at temperatures below 1720 K cannot be made due to the uncertainty in the surface condition of the samples and the amount of ^{95}Zr present in the ^{95}Nb isotope.

To measure diffusion in the homologous temperature range of the iron work (less than 1570 K), or to study isotope effects at lower temperatures, thin sections must be taken so that the anneal may be done in a reasonable length of time. The total profile would be less than 3 μm, and in most cases would be less than 1 μm. The impurity content of

this layer, not the bulk, must be known in order to compare diffusion rates in the oxygenated and the pure niobium.

At temperatures less than 1773 K, the surface cannot stay clean by evaporating oxides as it does at higher temperatures. Birnbaum[46] has indicated the temperature and pressure conditions necessary to keep a clean surface. When those conditions are not correct for evaporation of the oxide from the surface, oxygen is dissolved into the metal. This excess oxygen diffuses into the sample and finally equilibrates, but during the course of the anneal an oxygen gradient is in the exact place where it is most detrimental: the self-diffusion zone. Unfortunately, the condition of the surface layer changes as the niobium cools so the conditions measured on a cold sample can only be theoretically related to the sample at a higher temperature. Although a bulk analysis of the sample may indicate a low interstitial content, the surface layer may have a different impurity content.

B. Nonlinear Arrhenius behavior

Two models for explaining a curved Arrhenius plot are a temperature-dependent activation energy[47] and diffusion by a combination of single vacancies and divacancies. Isotope-effect measurements,[39] which unfortunately could not be made would help to identify the correct model. We have chosen to interpret the niobium self-diffusion data in terms of the prevalent single-vacancy–divacancy model. The nonlinear Arrhenius behavior found in vanadium self-diffusion[25] and in the niobium self-diffusion measurements reported here prompted a two-exponential analysis of recent data for self-diffusion in the three group-V bcc metals. The same variable metric minimization routine[48] was used for each set of data; the results are given in Table II. The activation energies for diffusion (Q) have been normalized by the melting temperature (T_m).

The values of all the parameters listed in Table II are considerably smaller than those found by similar analyses by Neumann[12] and by Mehrer *et al.*[13] The smaller values have particular significance if the two processes are interpreted in terms of single-vacancy and divacancy mechanisms. Direct evidence of diffusion by equilibrium vacancies in bcc refractory metals is not as strong as in fcc metals, but most analyses have been made assuming a vacancy model.[37,47] For a single-vacancy–divacancy model, the respective activation entropies for self-diffusion determined from the preexponential factors in Eq. (2) are $S_{1v} \sim 1k$ and $S_{2v} \sim 7k$. The previous analyses[12,13] yielded higher entropy factors. The values of the parameters for the group-V bcc metals given in Table II are similar to those found for the group-I fcc metals,[2,15,49] in which self-diffusion has been interpreted in terms of a single-vacancy–divacancy mechanism. The detailed analyses that have been possible for the fcc metals have allowed the determination of the formation enthalpy E_{1v}^F and migration enthalpy E_{1v}^M for single vacancies, and the binding energy E_{2v}^B and migration enthalpy E_{2v}^M of divacancies. For fcc metals, these parameters are related by the following equation

$$2E_{1v}^F - E_{2v}^B + E_{2v}^M = (Q_{2v}/Q_{1v})(E_{1v}^F + E_{1v}^M) . \quad (3)$$

In the case of the fcc metals that have been analyzed,[14,15,16] these parameters are related in the following manner: $E_{1v}^M/E_{1v}^F \sim 0.9$, $E_{2v}^B/E_{1v}^F \sim 0.25$, $E_{2v}^M/E_{1v}^F \sim 0.65$, and $Q_{2v}/Q_{1v} \sim 1.25$.

The similarity found for the diffusion parameters in the group-V and group-I metals could be fortuitous. If there is significance to the similarity in the diffusion parameters, then a much higher ratio of E_{1v}^M/E_{1v}^F than the previously suggested[37,47,50] value of ~0.25 for group-V metals would be expected. The low values have been obtained from quenching experiments, and one of the main difficulties of such investigations for group-V metals lies in their high sensitivity to interstitial contamination. However, the recent quenching experiments on high-purity niobium[51] would also yield a low value of E_{1v}^M/E_{1v}^F (~0.18). Equation (3) may not be applicable to bcc metals, because the number of different divacancy config-

TABLE II. Diffusion parameters in group V bcc metals.

Element	$(D_0)_1$ [a] ($cm^2\ sec^{-1}$)	$(D_0)_2$ [b] ($cm^2\ sec^{-1}$)	Q_1/T_m (cal/mole K)	Q_2/T_m (cal/mole K)	Q_2/Q_1	Reference
V	1.4×10^{-2}	7.5	31.2	39.8	1.27	25
Nb	8.0×10^{-3}	3.7	30.5	38.2	1.25	Present work
Ta	1.8×10^{-2}	10.0	28.7	37.7	1.32	19

[a] 1 represents single vacancies.
[b] 2 represents divacancies.

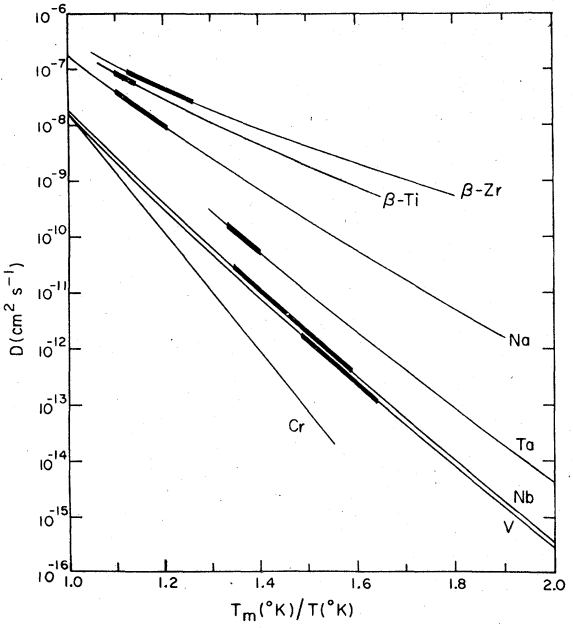

FIG. 6. Comparison of self-diffusion in bcc metals.

urations that are possible makes it difficult to define the ratio of the binding energy to migration energy of a divacancy. Measurements of the formation enthalpy of single vacancies would help to clarify this problem.

The present analyses of the group-V bcc metals, together with earlier analyses,[5,7,9] allow a comparison of all the bcc metals for which nonlinear Arrhenius behavior has been observed. The comparative data are plotted in Fig. 6, using a normalized temperature scale. On each curve, the thicker line indicates that region where the fitting procedure yields equal contributions to diffusion from the high-temperature and low-temperature processes, assuming that each can be represented by a linear Arrhenius behavior. There is a line of equal contribution instead of a point due to experimental uncertainty in the fitting procedure. These regions are farther from the melting temperature as the slope increases. There are no obvious physical grounds for this phenomenon. In terms of a single-vacancy–divacancy interpretation, the bcc metals would appear to have much larger divacancy contributions than the fcc metals, where divacancies contribute less than half to the diffusion coefficient at the melting point. On the basis of this empiricism, even the measurements on chromium self-diffusion[20] could have been expected to show nonlinear Arrhenius behavior at a much lower temperature. Empirically the phenomenon would also suggest that measurements of tungsten self-diffusion[22] have not been made to low enough temperatures to observe curvature in the Arrhenius plot.

ACKNOWLEDGMENTS

We wish to thank N. L. Peterson, S. J. Rothman, and R. W. Siegel for helpful discussions.

*Work supported by the U. S. ERDA.

†Present address: EBR-II Project, ANL-W, Idaho Falls, Id. 83401.

[1]H. Bakker, Phys. Status Solidi 28, 569 (1968).
[2]Nghi Q. Lam, S. J. Rothman, H. Mehrer, and L. J. Nowicki, Phys. Status Solidi B 57, 225 (1973).
[3]Nghi Q. Lam, S. J. Rothman, and L. J. Nowicki, Phys. Status Solidi A 23, K35 (1974).
[4]Chr. Herzig, H. Eckseler, and W. Bussman, International Conference on the Properties of Atomic Defects in Solids, Argonne National Laboratory, 1976 (unpublished).
[5]J. F. Murdock, T. S. Lundy, and E. E. Stansbury, Acta Metall. 12, 1033 (1968).
[6]J. F. Federer and T. S. Lundy, Trans. Metall. Soc. AIME 227, 592 (1963).
[7]J. N. Mundy, Phys. Rev. B 3, 2431 (1971).
[8]J. N. Mundy, T. E. Miller, and R. J. Porte, Phys. Rev. B 3, 2445 (1971).
[9]G. V. Kidson, Can. J. Phys. 41, 1563 (1963).
[10]R. F. Peart and J. Askill, Phys. Status Solidi 23, 263 (1967).
[11]A. Seeger and H. Mehrer, *Vacancies and Interstitials in Metals* (North-Holland, Amsterdam, 1969), p. 1.
[12]G. M. Neumann, *Diffusion Processes* (Gordon and Breach, London, 1971), p. 329.
[13]H. Mehrer, P. Kunz, and A. Seeger, Defects in Refractory Metals, International Conference Proceedings, Mol, 1972 (unpublished), p. 183.
[14]A. Seeger and H. Mehrer, Phys. Status Solidi 29, 231 (1968).
[15]H. Mehrer and A. Seeger, Phys. Status Solidi 35, 313 (1969).
[16]H. Mehrer and A. Seeger, Phys. Status Solidi 39, 647 (1970).
[17]K. Maier, H. Mehrer, E. Lessmann, and W. Schule, Phys. Status Solidi 78, 689 (1976).
[18]T. S. Lundy, F. R. Winslow, R. E. Pawel, and C. J. McHargue, Trans. Metall. Soc. AIME 233, 1533 (1965).
[19]R. E. Pawel and T. S. Lundy, J. Phys. Chem. Solids 26, 937 (1965).
[20]J. N. Mundy, C. W. Tse, and W. D. McFall, Phys. Rev. B 13, 2349 (1976).
[21]J. Askill and D. H. Tomlin, Philos. Mag. 8, 997 (1963).
[22]R. E. Pawel and T. S. Lundy, Acta. Metall. 17, 979 (1969).
[23]T. S. Lundy and C. J. McHargue, Trans. Metall. Soc. AIME 233, 243 (1965).
[24]R. F. Peart, J. Phys. Chem. Solids 26, 1853 (1965).
[25]J. Pelleg, Philos. Mag. 27, 383 (1974).
[26]R. E. Pawel and T. S. Lundy, J. Appl. Phys. 35, 435 (1964).

[27]R. E. Pawel, Rev. Sci. Instrum. 35, 1066 (1964).
[28]R. Resnick and L. S. Castleman, Trans. Metall. Soc. AIME 218, 307 (1960).
[29]R. F. Peart, D. Graham, and D. H. Tomlin, Acta Metall. 10, 519 (1962).
[30]V. D. Lyubimar, P. V. Gel'd, and G. P. Shoeybin, Izv. Akad. Nauk SSSR, Metall, Gorn. Delo 5, 137 (1964).
[31]G. B. Federov, F. I. Zhomov, and E. A. Smirnov, Metall. Metalloved. Chist. Met. 8, 145 (1969).
[32]V. Irmer and M. Feller-Kniepmeier, Philos Mag. 25, 1345 (1972).
[33]B. A. Loomis, A. T. Taylor, T. E. Klippert, and S. B. Gerber, Nucl. Metall. 18, 332 (1973).
[34]P. Mazot, Acta Metall. 21, 943 (1973).
[35]J. R. Manning, *Diffusion Kinetics for Atoms in Crystals* (Van Nostrand-Reinhold, Princeton, NJ, 1968).
[36]G. J. Jones and A. D. LeClaire, Philos. Mag. 26, 1191 (1972).
[37]H. Schultz, Mater. Sci. Eng. 3, 189 (1968/69).
[38]M. Strongin, H. H. Farrell, H. J. Halama, A. F. Kammerer, and C. Varmazis, Part. Accel. 3, 209 (1972).
[39]R. E. Einziger and J. N. Mundy, following paper, Phys. Rev. B 17, 449 (1978).
[40]H. K. Birnbaum (private communication).
[41]R. E. Einziger and J. N. Mundy, Rev. Sci. Instrum. 47, 1547 (1976).
[42]J. D. deVos, Physica 20, 690 (1954).
[43]R. C. Quinn, Br. J. Appl. Phys. 18, 1105 (1967).
[44]M. R. Arora and R. Kelly, Electrochimi. Acta 19, 413 (1974).
[45]K. Maier (private communication).
[46]H. K. Birnbaum, Scr. Metall. 7, 925 (1973).
[47]H. Gilder and D. Lazarus, Phys. Rev. B 11, 4916 (1975).
[48]M. Gabriel, ANL Report (unpublished).
[49]R. P. Sahu, K. C. Jain and R. W. Siegel, Properties of Atomic Defects in Metals, International Conference Proceedings, 1976 (unpublished).
[50]H. Schultz, Scr. Metall. 8, 721 (1974).
[51]K. Faber, J. Schweikhardt, and H. Schultz, Scr. Metall. 8, 713 (1974).